# Contrast-Free Transcranial Functional Ultrasound Neuroimaging

Emelina Vienneau\*, Abbie Weeks\*, Stephen Wilson<sup>†</sup>, Victoria Morgan<sup>‡</sup> and Brett Byram\*<sup>‡</sup>

\*Vanderbilt University School of Engineering

Vanderbilt University, Nashville, Tennessee, USA

<sup>†</sup>School of Health and Rehabilitation Science

University of Queensland, Brisbane, Australia

<sup>‡</sup>Radiology and Radiological Sciences Department

Vanderbilt University Medical Center, Nashville, Tennessee, USA

Abstract—Transcranial functional ultrasound is a relatively new technology for assessing functional responses in the brain. So far, transcranial functional ultrasound without contrast agents has only been applied to human imaging during surgery with the skull removed or in imaging neonates. Here, we demonstrate the feasibility of transcranial functional ultrasound through the adult skull. To overcome the severe attenuation from the skull we use a previously developed a compound Barker coded excitation method. For clutter filtering, we use an adaptive demodulation motion correction method with singular value decomposition (SVD) filtering. As a demonstration, we assess cerebrovascular reactivity induced by a breath hold. We measured the power Doppler signal in the vasculature surrounding the midbrain in a healthy adult volunteer during a five minute task of alternating free breathing and breath holding periods. We showed that the power Doppler signal in the blood vessels was highly correlated to the breath hold task ( $\rho$ =0.53) and the oxygen saturation ( $\rho$ =0.61) as measured by finger pulse oximeter. We also observed a delayed vasodilatory response in the power Doppler signal that reflected the delayed drop in oxygen saturation from the breath hold. These results demonstrate that contrast-free transcranial functional imaging in adults is possible using coded excitation to increase SNR and blood flow sensitivity and with appropriate motion compensation and clutter filtering techniques.

Index Terms—Ultrasound, Coded Excitation, Power Doppler, Functional Ultrasound, Functional Imaging

## I. Introduction

Functional ultrasound imaging (fUSI) is a promising new technology with many advantages over traditional competitors like fMRI, fNIRS or EEG [1]. To date, application of fUSI in adult humans has been restricted to scenarios without the skull because the high attenuation of the skull limits acoustic penetration and sensitivity to slow blood flow, making fUSI through the skull extremely challenging. Therefore, current human applications are limited to neonatal and intraoperative

The work of Emelina P. Vienneau was supported in part by the National Science Foundation Graduate Research Fellowship Program under Grant 1937963 and in part by the National Institute of Biomedical Imaging and Bioengineering under NIH Grant T32EB021937. The work of Brett C. Byram was supported in part by the National Institute of Biomedical Imaging and Bioengineering under NIH Grant R01EB020040; in part by the National Heart, Lung, and Blood Institute under Grant R01HL156034; and in part by the National Science Foundation CAREER Award under Grant IIS-1750994. He is also supported as the Hoy Family Faculty Fellow. Abbie Weeks is supported by the Vanderbilt Institute for Surgery and Engineering.

uses where the skull is not a limiting factor [2], [3]. Contrast-free transcranial fUSI would be a paradigm shift, opening up entirely new applications of ultrasound in the brain. In this work, we overcome skull attenuation using coded excitation and demonstrate contrast-free transcranial fUSI in a healthy adult subject.

To demonstrate feasibility we assess cerebrovascular reactivity—a measure of cerebrovascular health critical for brain injury patients that can be readily evaluated through a simple breath hold stimulus [4], [5]. This is a particularly useful task for assessing functional response using power Doppler because velocity by itself—as assessed by a modality such as transcranial pulsed wave doppler that measures velocity—is biased by the changing diameter of vessels in response to a stimulus such as breath hold [4].

## II. METHODS

## A. Data Acquisition Sequence

The data were acquired using an 8-transmit diverging wave synthetic aperture sequence. Each diverging wave had a subaperture of 15 elements and an opening angle of 90°. The diverging waves were separated by 7 elements. The pulse repetition frequency (PRF) between individual diverging waves was 4400 Hz, and the PRF between each set of 8 transmits was 550 Hz. Data were acquired for 1.2 seconds, which enabled a full power Doppler ensemble of 660 slow-time samples. The ensembles were repeated every 3 seconds. A high quality Focused B-Mode image with a 13 bit Barker code was acquired at the beginning of each acquisition.

The diverging wave transmissions were coupled with coded transmit excitation in order to boost signal-to-noise ratio (SNR). We used compound Barker codes combined with inverse filtering; a method we developed previously [6]. This particular coded excitation approach is attractive because it uses binary Barker codes that can be implemented without degradation on systems like the Verasonics that only feature tri-state transmit circuity. Additionally, compound Barker codes overcome the limited length of standard Barker codes, which max out at 13 bits. Compound Barker codes are constructed from Barker codes with the Kronecker product. They maintain the key property of having no spectral nulls, allowing

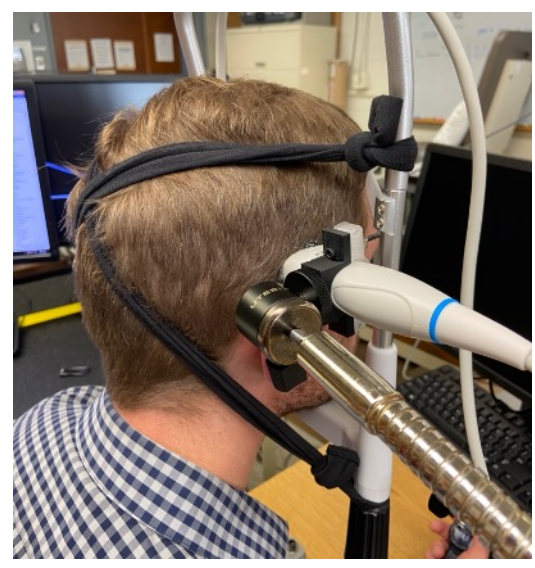


Fig. 1. The head rig is shown with a subject in place. The chin and forehead are placed in rests and cloth straps hold the head in place to minimize motion. The transducer is also held fixed relative to the rig using a custom fixation device.

stable inverse filters to be constructed for pulse compression with minimal artifacts (see the work of Vienneau and Byram for more details [6]). Here, we created a 65 bit compound code from 13 bit and 5 bit Barker codes, and we used a 256 tap FIR decoding filter for inverse filtering.

The sequence was implemented using a Verasonics Vantage system (Verasonics, Kirkland, WA, USA) with a P4-2v phased array transducer operating at 2.7 MHz.

# B. Functional Activation and Data Acquisition Protocol

Global functional neural activation in the brain was achieved using the previously mentioned breath hold stimulus. Breath hold is known to increase the cerebrovascular volumetric flow rate, and this approach has previously been visualized using MRI [5]. We acquired data over the course of a five minute long experiment with alternating periods of free breathing and breath holding. The first minute was a free breathing period and was used as a baseline power Doppler measurement. The power Doppler signal over the rest of the experiment was calculated as a percent change relative to this baseline period (% $\Delta$ PD). The baseline free breathing block was followed by a breath hold, free breathing, a breath hold, and free breathing, with each block lasting one minute. Oxygen saturation was also recorded during the experiment with a finger pulse oximeter.

Data for each protocol was acquired through the acoustic window in the temporal bone, and an imaging rig was used to help stabilize the transducer, which can be seen in Fig. 1. A subject places their chin and forehead into a dedicated head rest and an easily positioned arm held the transducer fixed against the acoustic window in the temporal bone.

# C. Data Processing Pipeline

The data processing largely used conventional methods. First, the compound Barker codes were compressed using

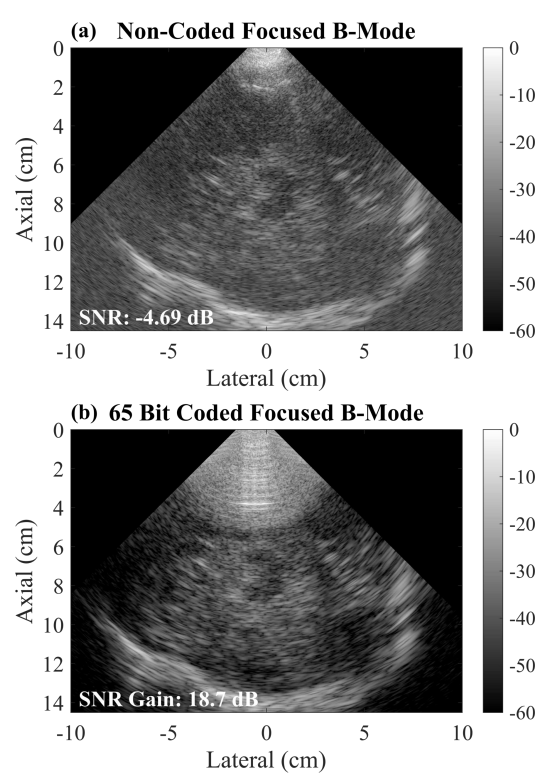


Fig. 2. This B-Mode pair shows an example with and without compound Barker coded excitation. The images qualitatively demonstrate the value of the coded excitation even for the B-Mode images. Additionally, this view is representative of the field view used for our acquisitions. The most recognizable structure is the mid-brain. The mid-brain is the primary anatomical structure used for orienting the field of view.

a pre-computed inverse filter applied to the channel data. Then, the remaining diverging wave transmit and receive sets were beamformed. After this, tissue clutter filtering was applied using a typical singular value decomposition (SVD) method combined with an adaptive tissue motion correction method [7]–[9]. Specifically, each windowed ensemble was processed with a SVD filter employing a single tissue cutoff to remove tissue clutter and a second cutoff to remove noise. This tissue cutoff was held constant for each windowed ensemble within a single protocol's data acquisition. The motion correction method was applied by estimating the motion using a  $10\lambda$  kernel and removing the estimated tissue displacement through subsample interpolation shifts.

The filtered data were used to create Power Doppler images. To assess functional activation, the Power Doppler images were compared to baseline levels determined by averaging the first minute of data and images were made to reflect  $\%\Delta\text{PD}$  relative this baseline. Pearson's correlation was computed between the  $\%\Delta\text{PD}$  within blood vessels and the block design of the experiment. Correlation was also computed between the blood vessel  $\%\Delta\text{PD}$  signal and the oxygen saturation curve.

### III. RESULTS

In Fig. 2 we show a B-mode image that is representative of our typical field of view. The mid-brain is visible in the middle of the image and the far side of the skull is visible at

the bottom of the image. We also show the image with and without a 65-bit code. This highlights the dead zone of the coded excitation transmit, which covers all of the near side of the skull and brain. (In the later processing the dead zone segment was cropped out.)

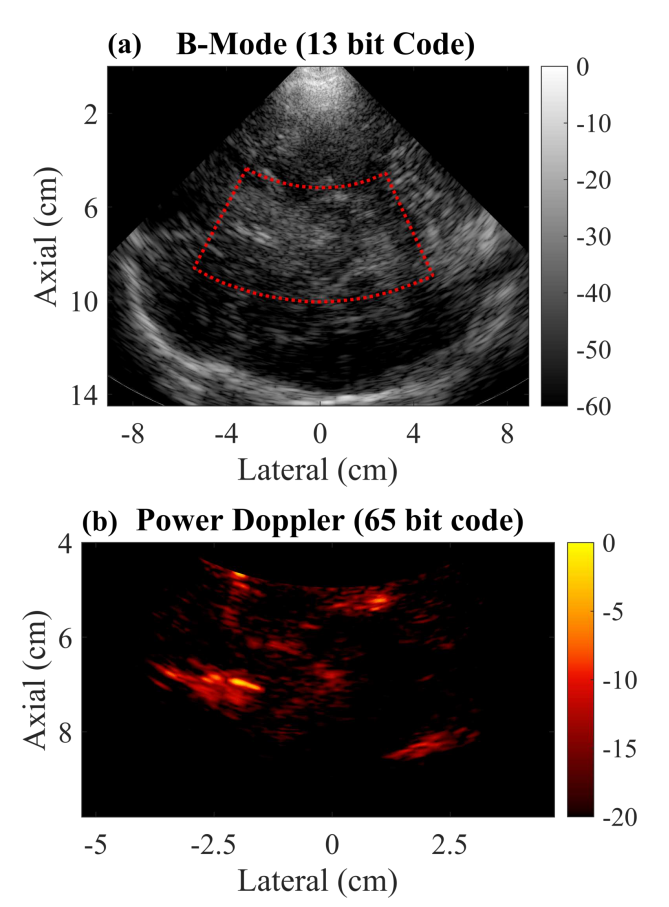


Fig. 3. This figure demonstrates an example power Doppler image from the region around the mid-brain.

We show an example power Doppler image in Fig. III. In the example, several vessels are easily visible around the midbrain. (The mid-brain itself is releatively unvascularized and appears dark in the power Doppler images.) It is also apparent in this particular subject that even with the coded transmit excitation the SNR drops off quickly as we get close to the far side of the skull at the bottom of the image. We did not quantitatively measure the SNR in this particular subject [10], but previous work measuring SNR in many subjects indicates that the SNR in this case is likely quite low and approaching 0 dB or lower towards the bottom of the image, resulting in the blood flow signal approaching the noise floor [11].

Next, we consider the results over time during our block design experiments. Fig. 4 shows the time series reflecting the change in power Doppler signal relative to the original baseline in the blood vessels during free breathing and breath hold blocks. Additionally, on each subfigure the Pearson's cross-correlation ( $\rho$ ) between the block design and the change in power Doppler signal is shown in the legend. The results highlight correlation in a range similar to what's observed by modalities like fMRI, which suggests that we are getting a

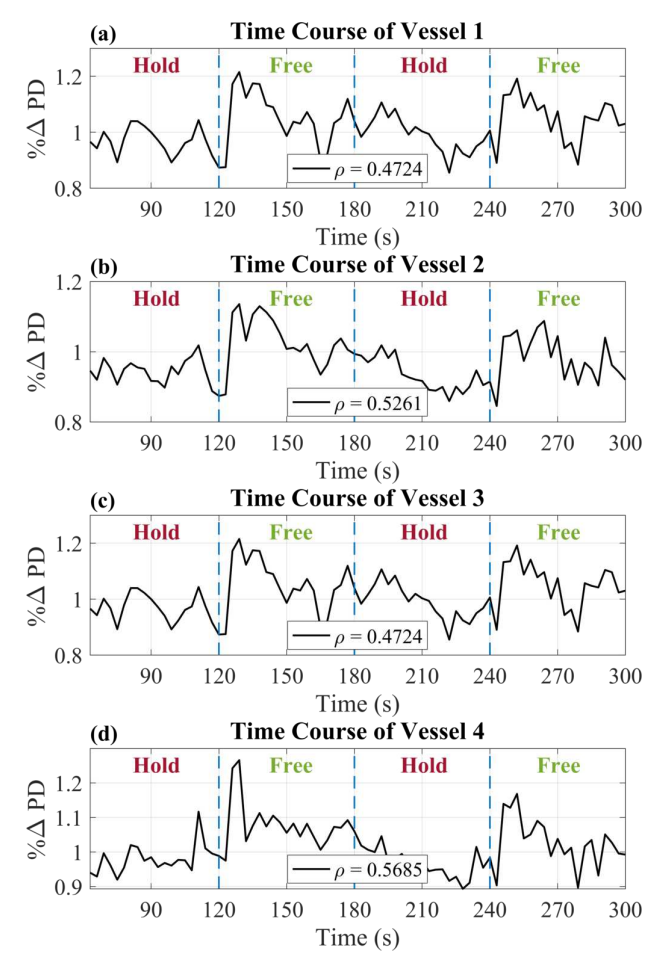


Fig. 4. The time series of the change in power Doppler signal for four different vessels from a single acquisition is shown. On each figure, the corresponding Pearsons's Cross-Correlation  $(\rho)$  is shown between  $\%\Delta PD$  and the block design.

reasonable functional response. This is also consistent with the expected change in cerebral blood volume during breath hold versus normal free breathing [5], [12]. We do note that there is a large delay in the functional response, which is partly due the neutral breath hold that was used. Breath holding at full expiration is known to produce a faster response and breath hold at full inspiration should produce an even slower response. The time delay of vasodilation also varies across subjects.

To provide further confirmation of the consistency of the response's delay, we compare the averaged power Doppler time series in the blood vessels to matched blood oxygen saturation measured with a pulse oximeter. This is shown in Fig. 5.

We note that the delayed vasodilatory response seen in the power Doppler data corresponds to the delayed drop in oxygen saturation from the breath hold. The oxygen saturation does not begin to drop until the end of the breath hold period and continues dropping further even after the breath hold release before suddenly overshooting to 100% saturation halfway through the next free breathing period. Correspondingly, the power Doppler data does not increase above baseline until

the beginning of the free breath period and then returns to baseline once the oxygen saturation recovers. In addition, we also note that the oxygen saturation drops lower after the first breath hold than the second, a feature which is also observed in the power Doppler data as the first peak in  $\%\Delta PD$  (around 124s) is higher than the second one (around 246s). Overall, these results confirm that we were able to capture clinically meaningful functional information using transcranial power Doppler imaging with coded excitation.

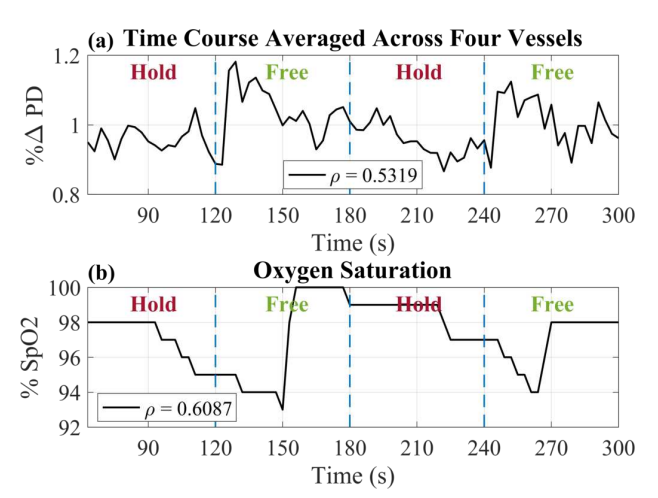


Fig. 5. The average of the power Doppler time series from the four vessels shown in Fig. 4 is compared to the corresponding pulse oximeter time series. Pearson's correlation coefficient ( $\rho$ ) between the blood vessel % $\Delta$ PD time series and the breath hold task is shown in the legend of the top panel. The correlation between the oxygen saturation curve and the blood vessel % $\Delta$ PD time series is shown in the legend of the bottom panel.

## IV. DISCUSSION AND CONCLUSIONS

Our results demonstrate that it is possible to detect a functional response in an adult brain with ultrasound transcranially. While, we are not seeing the small vascular trees visible in idealized scenarios without the skull and at higher imaging frequencies, we do reliably see small vessels around the highly vascularized mid-brain, and we are able to detect the corresponding vascular responses to a breath hold stimulus.

Here, we targeted the region around the mid-brain because we find that it is usually detectable even on relatively lowquality transcranial B-mode images through the temporal bone. However, with even slight improvements in reliable image quality, it will be relatively straightforward to target other brain regions. From our experience there are two primary impediments to accessibility. The first is the limit of what can be reached with a single 1D phased array transducer because adequate coupling is not maintained with more severe steering angles. In the future, 2D phase array transducers could better overcome this limitation. The second is the limit of the coded excitation. With long codes, there is a large dead zone that we show at shallow depths where the receive circuitry is saturated. Shorter codes reduce the size of the dead zone, but they may not provide a sufficient SNR boost to achieve adequate blood sensitivity. Therefore, structures from around the mid-brain to the far side of the skull are currently the most accessible, while maintaining some sense of anatomical orientation. This

could be overcome by either using a standoff pad between the transducer and the head or by imaging on both sides of brain in order to cover the full field of view.

In summary, we utilized our previously developed coded excitation technique to improve SNR and blood flow sensitivity in transcranial imaging, enabling us to perform contrast-free transcranial functional power Doppler imaging in an adult for the first time. With further refinements, this technology will be paradigm shifting and open up endless opportunities for ultrasound imaging in the brain.

### ACKNOWLEDGMENT

The authors gratefully acknowledge Dr. Adrian Jarquin-Valdivia for his guidance in transcranial ultrasound imaging and anatomy, and Joseph Howard for his assistance in developing the transcranial imaging rig.

#### REFERENCES

- [1] E. MacÉ, G. Montaldo, I. Cohen, M. Baulac, M. Fink, and M. Tanter, "Functional ultrasound imaging of the brain," *Nature Methods*, vol. 8, no. 8, pp. 662–664, aug 2011.
- [2] S. Soloukey, A. J. Vincent, D. D. Satoer, F. Mastik, M. Smits, C. M. Dirven, C. Strydis, J. G. Bosch, A. F. van der Steen, C. I. De Zeeuw, S. K. Koekkoek, and P. Kruizinga, "Functional Ultrasound (fUS) During Awake Brain Surgery: The Clinical Potential of Intra-Operative Functional and Vascular Brain Mapping," Frontiers in Neuroscience, vol. 13, jan 2020.
- [3] C. Demene, J. Baranger, M. Bernal, C. Delanoe, S. Auvin, V. Biran, M. Alison, J. Mairesse, E. Harribaud, M. Pernot, M. Tanter, and O. Baud, "Functional ultrasound imaging of brain activity in human newborns," *Science Translational Medicine*, vol. 9, no. 411, oct 2017.
- [4] N. S. Coverdale, J. S. Gati, O. Opalevych, A. Perrotta, and J. K. Shoemaker, "Cerebral blood flow velocity underestimates cerebral blood flow during modest hypercapnia and hypocapnia," *Journal of Applied Physiology*, vol. 117, no. 10, pp. 1090–1096, nov 2014.
- [5] A. Kastrup, T. Q. Li, G. H. Glover, and M. E. Moseley, "Cerebral blood flow-related signal changes during breath-holding," *American Journal of Neuroradiology*, vol. 20, no. 7, pp. 1233–1238, 1999.
- [6] E. P. Vienneau and B. C. Byram, "A Coded Excitation Framework for High SNR Transcranial Ultrasound Imaging," *IEEE Transactions on Medical Imaging*, pp. 1–13, 2023.
- [7] C. Demené, T. Deffieux, M. Pernot, B. F. Osmanski, V. Biran, J. L. Gennisson, L. A. Sieu, A. Bergel, S. Franqui, J. M. Correas, I. Cohen, O. Baud, and M. Tanter, "Spatiotemporal Clutter Filtering of Ultrafast Ultrasound Data Highly Increases Doppler and fUltrasound Sensitivity," *IEEE Transactions on Medical Imaging*, vol. 34, no. 11, pp. 2271–2285, nov 2015.
- [8] J. Tierney, K. Walsh, H. Griffith, J. Baker, D. B. Brown, and B. Byram, "Combining slow flow techniques with adaptive demodulation for improved perfusion ultrasound imaging without contrast," *IEEE Transactions on Ultrasonics, Ferroelectrics, and Frequency Control*, vol. 66, no. 5, pp. 834–848, may 2019.
- [9] J. Tierney, C. Coolbaugh, T. Towse, and B. Byram, "Adaptive clutter demodulation for non-contrast ultrasound perfusion imaging," *IEEE Transactions on Medical Imaging*, vol. 36, no. 9, pp. 1979–1991, sep 2017.
- [10] E. P. Vienneau, K. A. Ozgun, and B. C. Byram, "Spatiotemporal Coherence to Quantify Sources of Image Degradation in Ultrasonic Imaging," *IEEE Transactions on Ultrasonics, Ferroelectrics, and Frequency Control*, vol. 69, no. 4, pp. 1337–1352, apr 2022.
- [11] P. Song, A. Manduca, J. D. Trzasko, and S. Chen, "Ultrasound small vessel imaging with block-wise adaptive local clutter filtering," *IEEE Transactions on Medical Imaging*, vol. 36, no. 1, pp. 251–262, jan 2017.
- [12] A. Kastrup, T. Q. Li, A. Takahashi, G. H. Glover, and M. E. Moseley, "Functional magnetic resonance imaging of regional cerebral blood oxygenation changes during breath holding," *Stroke*, vol. 29, no. 12, pp. 2641–2645, 1998.